Inline Supplementary Figures

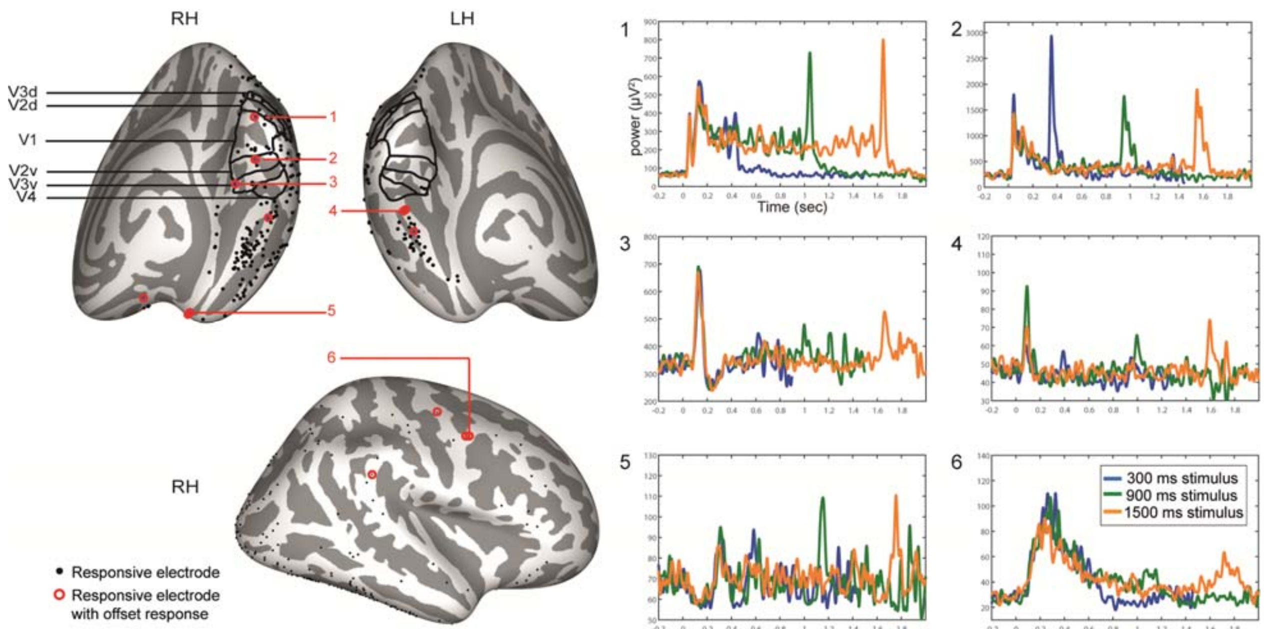

Figure S1: Responses to stimulus offset: Offset responses were found in 14 of the 292 responsive electrodes. Offset responses were detected based on a HFB power increase in the 300 ms post-stimulus time window compared to the preceding 300 ms window, as assessed by a cluster-based permutation test (Maris and Oostenveld, 2007). False-Detection Rate correction was applied (q=0.05) to define significant offset responses across all responsive electrodes. Offset responses were rare but not confined to a particular cortical region, and did not necessarily co-occur with sustained responses (compare for example electrodes 1 and 2). Left panel: electrodes with significant offset responses across all subjects and hemispheres. Right panel: examples for offset responses from the six numbered electrodes on the left panel.

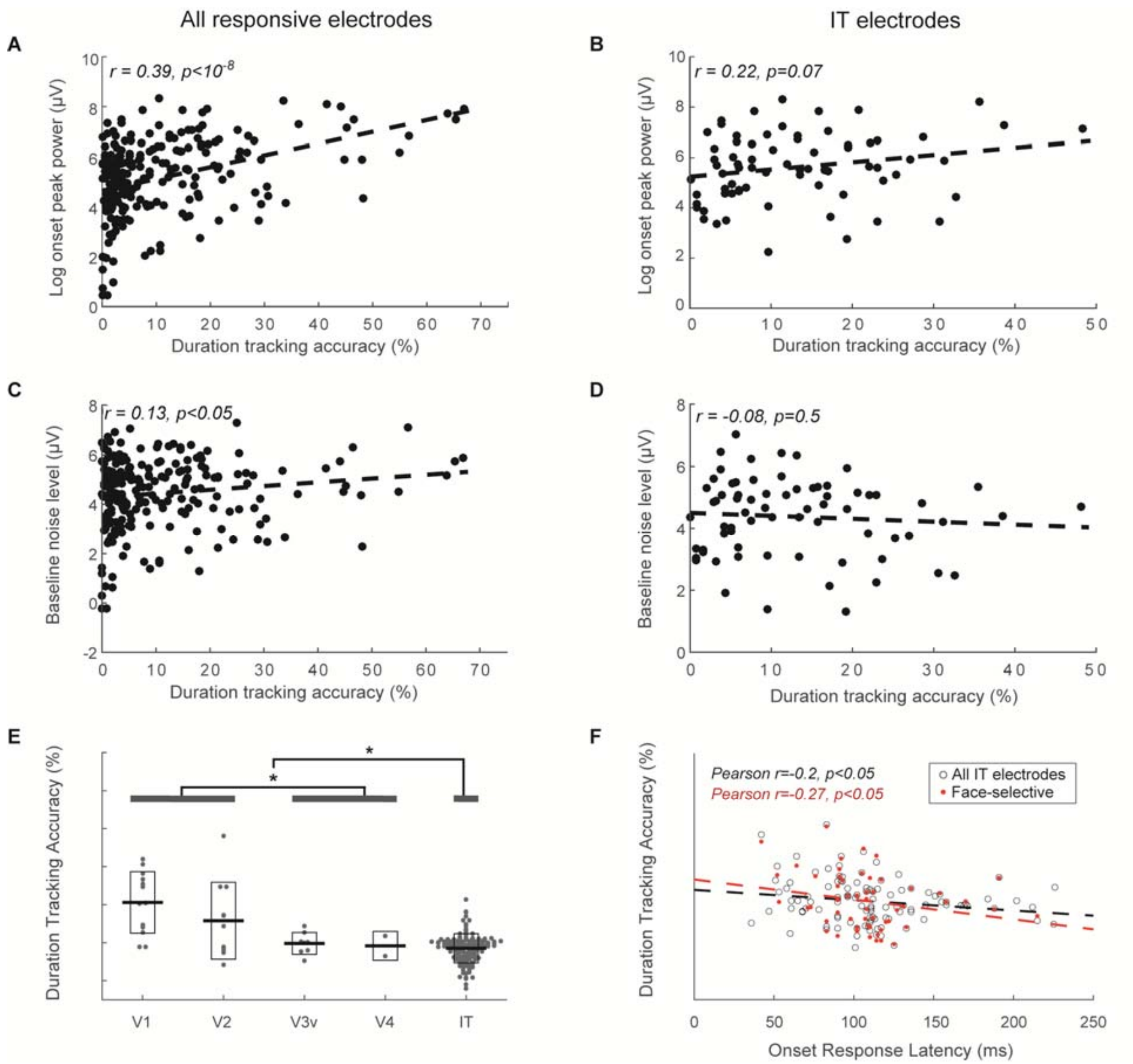

Figure S2: Controlling for baseline noise level and onset peak power. (**A, B**) the signal-to-noise ratio (SNR) of each electrodes' HFB onset response, measured as the log of the ratio between the peak power of the 0-300 ms epoch in the average response for the preferred stimulus category (or for all categories for non-selective electrodes) and the standard deviation of the baseline, is correlated with duration-tracking accuracy across all right-hemisphere visually-responsive electrodes and across IT electrodes. (**C,D**) the baseline noise level for each electrode, measured as the log of the standard deviation of the baseline HFB power, is also mildly correlated with accuracy. Despite their correlation with duration-tracking accuracy, onset SNR and baseline noise level factors do not explain the negative correlation between duration-tracking accuracy and hierarchical position along the ventral stream. This was verified by regressing out the variance in the accuracy variable explained by these two factors using multiple regression, and analyzing the residual variance. As in the original analysis, accuracy was higher in EVC areas than in IT ($t(166)=7.2$, $p<10^{-5}$), and in V1/V2 than V3v/V4 ($t(32)=2.9$, $p<0.01$; panel (**E**)**,** compare to Fig 1C), and within inferior temporal electrodes duration accuracy inversely correlated with response latency (panel (**F**), compare to Fig 1D). Correlating accuracy with position along the posterior-anterior axis produced comparable results (r=-0.31, p<0.01 for all IT electrodes, r=-0.36, p<0.01 for face-selective electrodes).

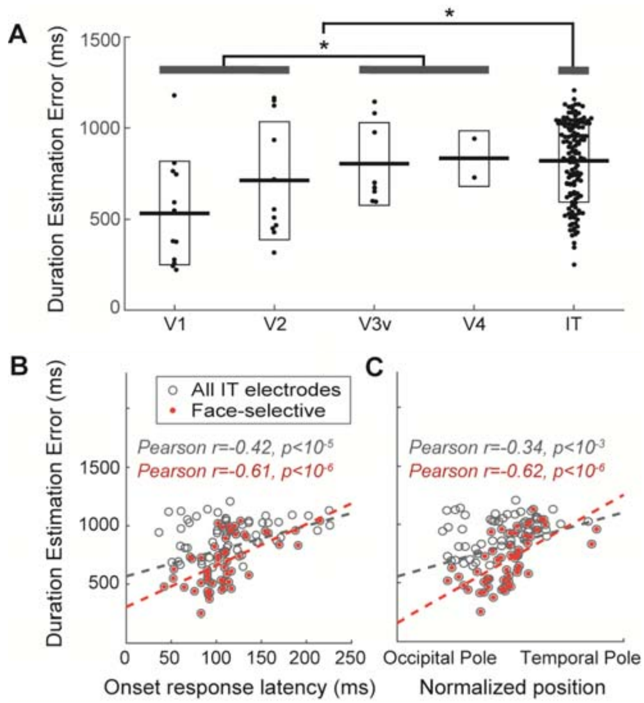

Figure S3. Duration tracking estimation error. To verify that the effects reported for duration-tracking accuracy were not dependent on the particular accuracy metric used, the same results reported in Fig 1 were replicated using the mean duration estimation error as the dependent variable. (**A**) Relation between duration estimation error and hierarchical position along the ventral stream, based on a probabilistic atlas (EVC areas) and visual inspection (IT). Boxes correspond to standard deviation. Error in EVC areas is lower than in IT (t(166)=-3.2, p<0.01), and in V1/V2 compared to V3v/V4 (t(32)=-1.82, p<0.05). (**B**) duration-tracking within IT as a function of onset response latency as a proxy for hierarchical position along the ventral stream. (**C**) Same as (B), with hierarchical position measured as the electrode's coordinate along the occipital-temporal axis.

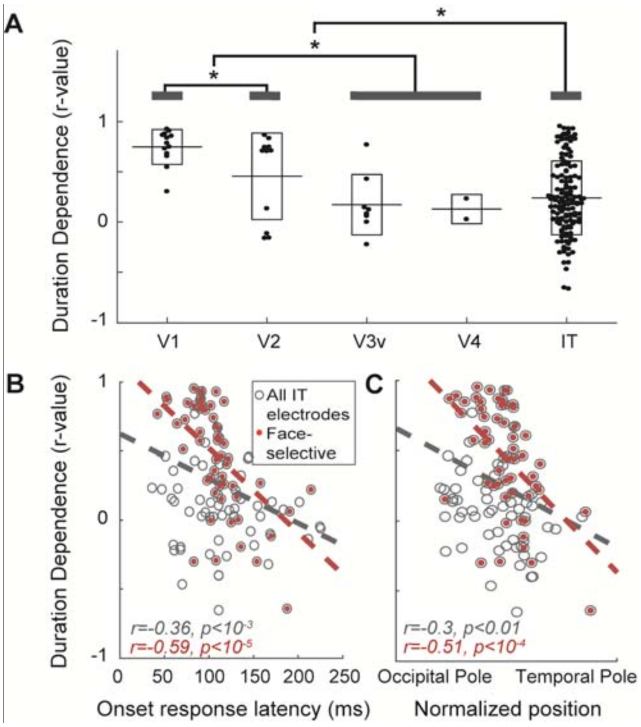

Figure S4. Decreasing duration dependence along the ventral stream. (**A**) The duration-dependence index (i.e., the correlation across trials between number of post-stimulus above-baseline time points and stimulus duration) as a function of region, plotted for all visually-responsive electrodes. Boxes indicate standard deviation. Duration dependence is higher in EVC areas than in IT ($t(166)=3.4$, $p<10^{-3}$), in V1/V2 than in V3v/V4 ($t(32)=3.68$, $p<10^{-3}$), and in V1 than in V2 ($t(22)=2.25$, $p<0.05$). (**B**) Duration dependence within IT as a function of onset response latency. (**C**) Duration dependence within IT as a function of anatomical position along the posterior-anterior axis.